

Spatial-Temporal Decoupling Contrastive Learning for Skeleton-based Human Action Recognition

Shaojie Zhang¹, Jianqin Yin^{1,2*}, Yonghao Dang¹

¹Beijing University of Posts and Telecommunications

²Queen Mary School Hainan, Beijing University of Posts and Telecommunications

{zsj, jqyin, dyh2018}@bupt.edu.cn

Abstract

Skeleton-based action recognition is a central task of human-computer interaction. However, most of the previous methods suffer from two issues: (i) semantic ambiguity arising from spatiotemporal information mixture; and (ii) overlooking the explicit exploitation of the latent data distributions (*i.e.*, the intra-class variations and inter-class relations), thereby leading to local optimum solutions of the skeleton encoders. To mitigate this, we propose a spatial-temporal decoupling contrastive learning (STD-CL) framework to obtain discriminative and semantically distinct representations from the sequences, which can be incorporated into almost all previous skeleton encoders and have no impact on the skeleton encoders when testing. Specifically, we decouple the global features into spatial-specific and temporal-specific features to reduce the spatiotemporal coupling of features. Furthermore, to explicitly exploit the latent data distributions, we employ the attentive features to contrastive learning, which models the cross-sequence semantic relations by pulling together the features from the positive pairs and pushing away the negative pairs. Extensive experiments show that STD-CL with four various skeleton encoders (HCN, 2S-AGCN, CTR-GCN, and Hyperformer) achieves solid improvement on NTU60, NTU120, and NW-UCLA benchmarks. The code will be released at <https://github.com/LibertyZsj/STD-CL>.

1 Introduction

Human action recognition is an active task in the computer vision area. Due to its wide range of applications in human-computer interaction, video analysis, virtual reality, and so on, this task has been researched extensively in the past decade [Ren *et al.*, 2020]. In recent years, with the development of depth sensors [Cao *et al.*, 2017] and human pose estimation algorithms [Dang *et al.*, 2019], the skeleton sequence consisting of coordinates of human joints can be easily acquired. The skeleton-based action recognition utilizing

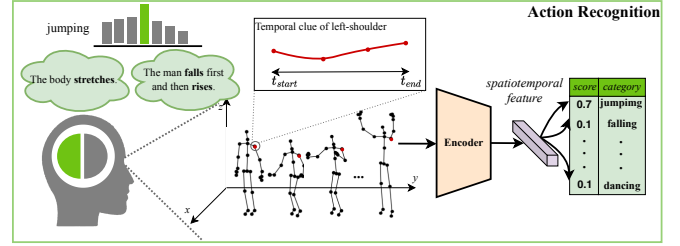


Figure 1: The framework of action recognition in both the perspective of humans and Deep Neural Network (DNN).

human joints has attracted much interest due to its robustness to background clutter, illumination, and viewpoint changes [Zhang *et al.*, 2019].

Generally, most of the previous approaches [Shi *et al.*, 2019; Chen *et al.*, 2021a; Chen *et al.*, 2021b] in skeleton-based action recognition follow a paradigm as shown in Figure 1. A skeleton encoder extracts the spatiotemporal co-occurrence feature [Li *et al.*, 2018], and a softmax-based linear classifier is used to project the feature to the category distributions. However, this paradigm has some limitations. The main problems are the fine-grained semantic ambiguity arising from the spatiotemporal information mixture in the co-occurrence feature and the absence of explicit exploitation of the latent data distributions.

When a person performs a certain action, the movements of joints occur concurrently in spatial and temporal dimensions, which results in the spatiotemporal coupling of the action. The global features extracted from the skeleton encoders mix the spatiotemporal information, which leads to a mixture of spatial-specific and temporal-specific features, each reflecting distinct semantics at the corresponding dimension. For example, when distinguishing the actions "put on a hat" and "take off a hat", which differ more in the frame-level dimension, temporal-specific information is more important. Conversely, the actions "point to something" and "throw", have more spatial differences in the joint-level dimension, so spatial-specific information is more important to distinguish them. **The features with clear spatio-temporal information are beneficial for distinguishing fine-grained actions.**

Specifically, an action can be composed of a series of sub-

*Corresponding Author

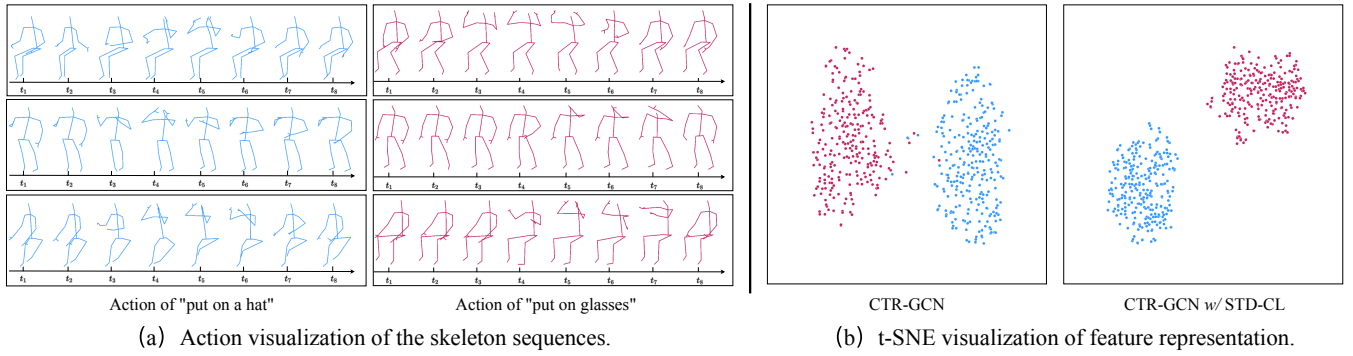


Figure 2: (a) Visualization of action "put on a hat" (left) and "put on glasses" (right) performed by different persons in the same view. (b) Visualization of feature representation by t-SNE for the corresponding action in the test set. The left one is from the CTR-GCN, while the right one is from our method. Each color denotes a certain class.

actions along the temporal dimension. As shown in Figure 2 (a), both the action "put on a hat" and the action "put on glasses" contain a crucial sub-action "lift the arms". Thus, the actions exhibit a degree of semantic similarity, leading to less distinct inter-class distances. Furthermore, due to the diversity in the external environment and individual differences, actions within the same category exhibit intra-class variation. The linear classifier is typically trained to optimize accuracy only, paying less attention to exploiting the latent data distributions. As shown in Figure 2 (b), the t-SNE distribution visualization of features extracted from CTR-GCN can't locate a distinguishable classification boundary. The absence of explicit modeling of the intra-class variation and inter-class relation may lead to confusion in recognizing ambiguous samples. Therefore, **the explicit exploitation of the latent data distributions is vital for recognizing the ambiguous sequences.**

To alleviate these drawbacks, we propose a spatial-temporal decoupling contrastive learning (STD-CL) framework to encourage the skeleton encoders to learn more discriminative and semantically distinct representations. It's worth noting that our STD-CL could be combined with previous skeleton encoders and have no impact on the skeleton encoders when testing. In the **training** phase, the global features are decoupled into spatial attentive features and temporal attentive features through the designed spatial-temporal feature decoupling (STFD) module. Moreover, we build two memory banks to store the decoupled spatial and temporal features respectively, and sample the positives and negatives from them according to labels. In particular, we employ contrastive learning to model the cross-sequence semantic relations by pulling together the decoupled features from positive pairs and pushing away the features from negative pairs. With constant contrast, the skeleton encoders are forced to explicitly the latent data distributions with distinct inter-class relations and reduced intra-class variations. Meanwhile, since the features used for contrast are decoupled, the degree of spatiotemporal information coupling within global features decreases so that the semantics become more explicit. Moreover, in the **testing** phase, the skeleton encoders can directly predict the categories with higher accuracy.

Overall, our main contributions can be summarized as follows:

- To extract more discriminative and semantically distinct features from the skeleton sequences, we proposed a novel STD-CL framework to decouple the features into spatial- and temporal-specific features and apply them for contrastive learning to explore the latent data distributions.
- The proposed STD-CL can be seamlessly incorporated into most previous skeleton encoders, which can be regarded as plug-and-play in the training stage and has no impact at the testing stage.
- Extensive experiments show that STD-CL achieves significant improvements based on four various state-of-the-art methods (HCN [Li *et al.*, 2018], 2S-AGCN [Shi *et al.*, 2019], CTR-GCN [Chen *et al.*, 2021a], and Hyperformer [Zhou *et al.*, 2022]) on three benchmark datasets (NTU60, NTU120, and NW-UCLA).

2 Related Work

2.1 Skeleton-based Action Recognition

Skeleton-based action recognition aims to classify actions from sequences of human keypoints. In early studies, RNN was a natural choice to handle the skeleton sequence. HBRNN [Du *et al.*, 2015] applied a hierarchical RNN architecture to model the long-range temporal dependency of the skeleton sequences. STA-LSTM [Song *et al.*, 2017] proposed an end-to-end spatial and temporal attention model to focus on discriminative joints of the skeleton within each frame of the inputs. Inspired by the success of CNN in image recognition, CNN-based methods have also been studied. HCN [Li *et al.*, 2018] treated the joint dimension as channels to aggregate different levels of spatiotemporal context information. TA-CNN [Xu *et al.*, 2022] adopted a pure CNN architecture to model the irregular skeleton topology.

The human body can be abstracted as a graph structure, which treats the joint as a node and the bone between two joints as an edge. Thus, GCN-based methods were introduced to this task. ST-GCN [Yan *et al.*, 2018] adopted GCN

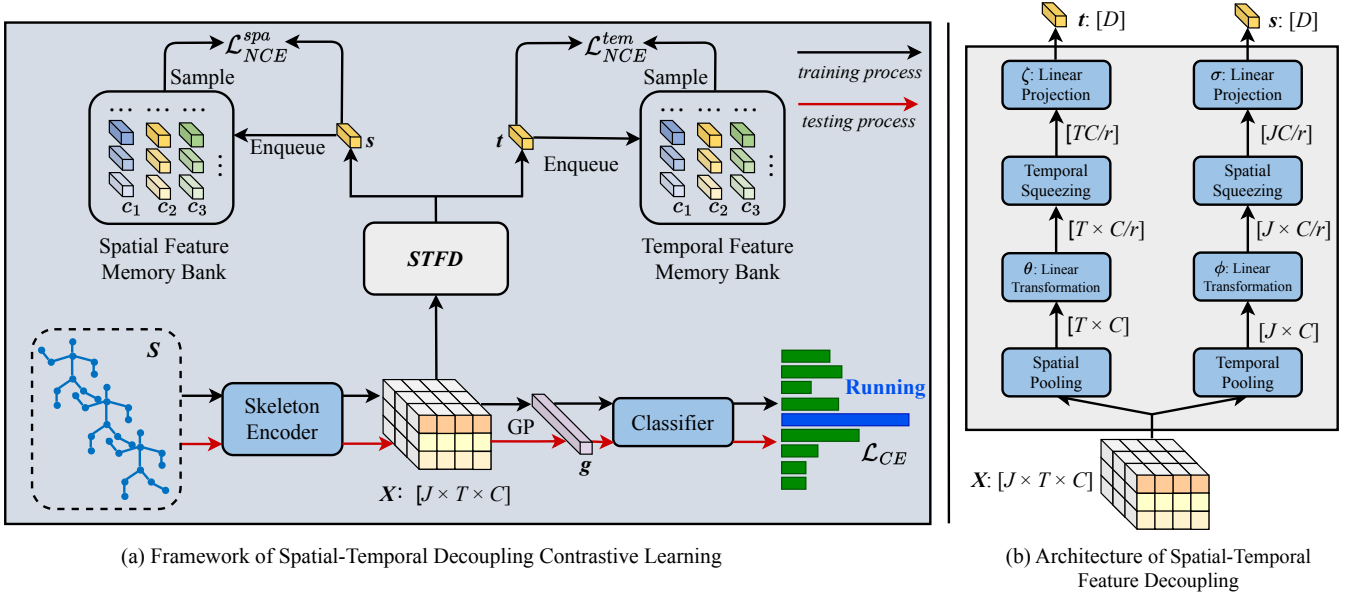


Figure 3: Overview of the proposed methods. The black line represents the training process and the red line represents the testing process. (a) The framework of our proposed Spatial-Temporal Decoupling Contrastive Learning (STD-CL). The skeleton encoder extracts spatiotemporal feature X from the input skeleton sequence S . Then the feature X is fed into the Spatial-Temporal Feature Decoupling (STFD) module to decouple spatial attentive feature s and temporal attentive feature t . Two memory banks are built to store the decoupled features respectively. We contrast the positive and negative instance features sampled from the memory banks according to the labels. The memory banks and the contrastive learning process are only used in the training phase and have no impact in the testing phase. (b) The architecture of the STFD module.

on the predefined spatial-temporal graphs to model the relations between joints. 2S-AGCN [Shi *et al.*, 2019] modeled the correlation between two joints given corresponding features with the self-attention mechanism. CTR-GCN [Chen *et al.*, 2021a] proposed a channel-wise topology refinement graph convolution to model fine-grained relation. InfoGCN [Chi *et al.*, 2022] combined a learning objective and an encoding method to break the information bottleneck.

With the popularity of transformers in computer vision, transformer-based methods have also been investigated for this task. ST-TR [Plizzari *et al.*, 2021] proposed a two-stream transformer architecture to model the spatial and temporal dimensions respectively. Hyperformer [Zhou *et al.*, 2022] applied transformer to model spatiotemporal features from the hyper-graph of the sequences.

2.2 Contrastive Learning

Recently, contrastive learning has been widely used in self-supervised representation learning. The core idea is to learn the discriminative features by pulling the positive pairs and pushing away the negative pairs in the embedded space. The positive pairs are features from transformed sample versions with different augmentations, and the negative pairs are from different samples. InstDisc [Wu *et al.*, 2018] maintained a memory bank for storing representations. SimCLR [Chen *et al.*, 2020] proposed to adopt a huge batch size to learn more useful representations. MoCo [He *et al.*, 2020] built a dynamic dictionary with a momentum update based on a memory bank to keep the stored representations consistent.

Inspired by this, our work tries to introduce memory bank mechanisms for contrastive learning to obtain discriminative features.

Contrastive learning was usually adopted in prior works [Xu *et al.*, 2023] to learn the invariance from the skeleton sequences for unsupervised learning in this field. Moreover, several works are applying contrastive learning to supervised action recognition. GAP [Xiang *et al.*, 2023] proposed a framework for contrasting the features from visual and text modalities to enhance the representation by using knowledge about actions and human body parts. SkeletonGCL [Huang *et al.*, 2023] explicitly explored the rich cross-sequence relations by using graph contrastive learning. However, SkeletonGCL can only be incorporated into the GCN-based methods, which limits its generalization. FR-Head [Zhou *et al.*, 2023] employed multi-level contrastive learning in GCN-based methods to distinguish ambiguous actions.

However, the methods mentioned above are more like surgery for GCN-based skeleton encoders, leading to limitations on generalizability to other types of methods.

3 Methodology

3.1 Preliminary

Notations

In our work, bold-face lower/upper-case letters denote vectors and tensors, respectively, and light-face lower/upper-case letters mean scalars.

Background

Skeleton-based action recognition is to predict the categories from the input sequences. We define the human skeleton sequence with J keypoints and T_0 frames in 3D space as $S \in \mathbb{R}^{J \times T_0 \times 3}$. The sequence is fed into a skeleton encoder \mathcal{F} to extract the features $X \in \mathbb{R}^{J \times T \times C}$. The skeleton encoder aggregates spatial and temporal information to obtain discriminative spatiotemporal features. After fully spatiotemporal aggregations, a global pooling (GP) layer is adapted to summarize the global features. Finally, a softmax-based fully-connected (FC) layer maps the global feature to a probability prediction $\hat{y} \in \mathbb{R}^K$ of K candidate categories. The process can be defined as:

$$X = \mathcal{F}(S) \quad (1)$$

$$y = FC(GP(X)) \quad (2)$$

In the process of optimization, a standard cross-entropy loss is applied to supervise the prediction distribution and the ground truth y as follows:

$$\mathcal{L}_{CE} = - \sum_i y_i \log \hat{y}_i \quad (3)$$

3.2 Spatial-Temporal Decoupling Contrastive Learning

Human actions have the property of spatio-temporal coupling, the feature X after extraction contains complex spatial and temporal relations, which may mix the spatial and temporal information. Thus, we decouple the feature to spatial attentive feature and temporal attentive feature to reduce the spatiotemporal information coupling. To further obtain more discriminative features we apply the decoupled features to contrastive learning to explore the cross-sequence semantic relations. The core is to explore the latent data distributions by pulling together the features from the positive pairs and pushing away the negative pairs.

Spatial Temporal Feature Decoupling

The details of the proposed STFD are shown in (b) of Figure 3. The feature X is fed into two parallel branches for feature decoupling. In the spatial feature decoupling (SFD) module, a temporal pooling layer is adopted to obtain the spatial attentive feature $X_s \in \mathbb{R}^{J \times C}$. And the temporal attentive feature $X_t \in \mathbb{R}^{T \times C}$ is obtained through a spatial pooling layer. Then, two linear transformation functions θ and ϕ with a channel reduction rate of r are used to transform the attentive features into a neatly compact representation as follows:

$$\begin{cases} X_s^* = \theta(X_s) = X_s W_\theta \in \mathbb{R}^{J \times C/r} \\ X_t^* = \phi(X_t) = X_t W_\phi \in \mathbb{R}^{T \times C/r} \end{cases} \quad (4)$$

where, $W_\theta, W_\phi \in \mathbb{R}^{C \times C/r}$ are the weights of the spatial and temporal transformation function, respectively. After this, to retain the attentive information, we squeeze the spatial dimension into the channel dimension in the SFD module, and the TFD module is similar. In the end, two liner transformation functions ζ and σ are used to transform the features to

the latent space for further contrastive learning, which can be formulated as:

$$\begin{cases} s = \zeta(s^*) = s^* W_\zeta \in \mathbb{R}^D \\ t = \sigma(t^*) = t^* W_\sigma \in \mathbb{R}^D \end{cases} \quad (5)$$

where, $W_\zeta \in \mathbb{R}^{JC/r \times D}$, $W_\sigma \in \mathbb{R}^{TC/r \times D}$ are the weights of final projection function. In this way, we decouple the spatial attentive feature s and the temporal attentive feature t from the spatiotemporal feature X .

Memory Bank

To obtain abundant negative pairs, we contrast two memory banks \mathcal{M}_{spa} and \mathcal{M}_{tem} to store the decoupled attentive features. Specifically, to avoid introducing hyperparameters and encourage the model to explore the cross-sequence context fully, we set the two memory banks to store the attentive features of all samples. Thus, the memory banks $\mathcal{M}_{spa}, \mathcal{M}_{tem} \in \mathbb{R}^{L \times D}$. L is the number of the instance of the dataset. When an instance is fed into the model to extract features, the stored features in the memory banks are updated according to the corresponding index.

$$\begin{cases} \mathcal{M}_{spa}[i] = s_i \\ \mathcal{M}_{tem}[i] = t_i \end{cases} \quad (6)$$

where i is the index of the instance in the dataset. Each element in \mathcal{M}_{spa} and \mathcal{M}_{tem} indicates a decoupled feature embedding from an instance. In the memory banks, the corresponding labels with the decoupled features are stored for the feature selection. Particularly, the decoupled features with the same category label as the current instance are selected as positive pairs, and negative pairs are sampled from the memory banks with other labels.

Training Objective

The positive pairs and negative pairs sampled from the two memory banks are used to achieve spatial-temporal decoupled contrastive learning. To pull together the positive pairs and push away the negative pairs, we define the distances between the two vectors with cosine similarity as follows:

$$\langle u, v \rangle = \frac{u \cdot v^T}{\|u\| \|v\|} \quad (7)$$

where u, v are the features sampled from the memory banks. Then the InfoNCE loss adopted for spatial-specific feature contrasting and temporal-specific feature contrasting can be written as follows:

$$\mathcal{L}_{NCE}^{spa} = - \sum_{s^+ \in \mathcal{M}_{spa}^+} \log \frac{\langle s, s^+ \rangle / \tau}{\sum_{s^- \in \mathcal{M}_{spa}^-} \langle s, s^- \rangle / \tau} \quad (8)$$

$$\mathcal{L}_{NCE}^{tem} = - \sum_{t^+ \in \mathcal{M}_{tem}^+} \log \frac{\langle t, t^+ \rangle / \tau}{\sum_{t^- \in \mathcal{M}_{tem}^-} \langle t, t^- \rangle / \tau} \quad (9)$$

where τ is a temperature hyperparameter in contrastive learning. \mathcal{M}_{spa}^+ and \mathcal{M}_{tem}^+ are the sets of the decoupled features from the positive sequences with the same label as the current

Table 1: Top-1 action acsification accuracy comparison (%) with the state-of-the-art methods on NTU 60 and NTU120 datasets. The numbers in gray indicate the results reported in their papers. Particularly, the 2S incidents the ensemble results of *joint* and *bone* streams. And the 4S incidents the ensemble results of *joint*, *bone*, *joint motion* and *bone motion* streams. * denotes the ensemble results of the streams reported in their papers.

Dataset Setting Method/Streams	NTU 60								NTU 120							
	X-Sub				X-View				X-Sub				X-Set			
	<i>J</i>	<i>B</i>	2S	4S	<i>J</i>	<i>B</i>	2S	4S	<i>J</i>	<i>B</i>	2S	4S	<i>J</i>	<i>B</i>	2S	4S
VA-LSTM [Zhang <i>et al.</i> , 2017]	-	-	79.4*	-	-	-	87.6*	-	-	-	-	-	-	-	-	-
AGC-LSTM [Si <i>et al.</i> , 2019]	-	-	89.2*	-	-	-	95.0*	-	-	-	-	-	-	-	-	-
ST-GCN [Yan <i>et al.</i> , 2018]	81.5	-	-	-	88.3	-	-	-	-	-	-	-	-	-	-	-
SGCN [Zhang <i>et al.</i> , 2020]	-	-	89.0	-	-	-	94.5	-	-	-	79.2	-	-	-	81.5	-
Shift-GCN [Cheng <i>et al.</i> , 2020b]	87.8	-	89.7	90.7	95.1	-	96.0	96.5	80.9	-	85.3	85.9	83.2	-	86.6	87.6
DC-GCN+ADG [Cheng <i>et al.</i> , 2020a]	-	-	90.8	-	-	-	96.6	-	-	-	86.5	-	-	-	88.1	-
Dynamic GCN [Ye <i>et al.</i> , 2020]	-	-	-	91.5	-	-	-	96.0	-	-	-	87.3	-	-	-	88.6
MS-G3D [Liu <i>et al.</i> , 2020]	89.4	90.1	91.5	-	95.0	95.3	96.2	-	-	-	86.9	-	-	-	88.4	-
DSTA [Shi <i>et al.</i> , 2020]	-	-	91.5	-	-	-	96.4	-	-	-	86.6	-	-	-	88.0	-
MST-GCN [Chen <i>et al.</i> , 2021b]	89.0	89.5	91.1	91.5	95.1	95.2	96.4	96.6	82.8	84.8	87.0	87.5	84.5	86.3	88.3	88.8
ST-TR [Plizzari <i>et al.</i> , 2021]	-	-	89.9	-	-	-	96.1	-	-	-	82.7	-	-	-	84.7	-
TA-CNN [Xu <i>et al.</i> , 2022]	88.9	89.2	91.0	91.5	94.5	94.1	95.7	95.9	84.0	85.1	87.8	88.2	85.3	86.3	89.0	89.6
EfficientGCN-B4 [Song <i>et al.</i> , 2022]	-	-	91.7	-	-	-	95.7	-	-	-	88.3	-	-	-	89.1	-
InfoGCN [Chi <i>et al.</i> , 2022]	89.4	90.6	91.3	92.3	95.2	95.4	96.2	96.7	84.2	86.9	88.2	89.2	86.3	88.5	89.4	90.7
HCN [Li <i>et al.</i> , 2018]	-	-	84.3*	-	-	-	89.9*	-	-	-	-	-	-	-	-	-
HCN w/ STD-CL	-	-	85.1*	-	-	-	91.2*	-	-	-	-	-	-	-	-	-
2S-AGCN [Shi <i>et al.</i> , 2019]	88.9	89.2	91.0	91.5	94.5	94.1	95.7	95.9	83.8	84.9	87.7	88.1	85.6	86.4	89.0	89.8
2S-AGCN w/STD-CL	89.4	89.8	91.5	91.9	94.7	94.6	96.1	96.3	84.1	85.1	87.9	88.2	86.0	86.3	89.2	89.6
CTR-GCN [Chen <i>et al.</i> , 2021a]	89.8	90.2	92.0	92.4	94.8	94.8	96.3	96.8	84.9	85.7	88.7	88.9	86.7	87.5	90.1	90.5
CTR-GCN w/STD-CL	90.4	90.8	92.2	92.7	95.2	95.0	96.4	96.9	85.5	86.7	89.3	88.9	86.8	88.2	90.4	90.5
Hyperformer [Zhou <i>et al.</i> , 2022]	90.3	91.1	92.0	92.7	94.5	94.4	95.5	96.2	86.1	87.4	88.9	89.9	87.8	89.0	90.6	91.2
Hyperformer w/STD-CL	90.8	91.3	92.3	-	95.0	94.7	95.9	-	86.8	88.1	89.2	-	-	-	-	-

feature in the memory banks. \mathcal{M}_{spa}^- and \mathcal{M}_{tem}^- are the sets of negative features with different lalbes.

Finally, the total training loss function of our proposed STD-CL is defined as follows:

$$\mathcal{L} = \mathcal{L}_{CE} + \mathcal{L}_{NCE}^{spa} + \mathcal{L}_{NCE}^{tem} \quad (10)$$

Sampling Strategy

To achieve efficient contrast across sequences, the strategy for sampling features from memory banks for contrastive learning has a large impact on the experimental performance. Therefore, in this paper, we follow the sampling strategy in [Huang *et al.*, 2023], which combines the hard mining strategy and random sampling strategy. The hard mining strategy is introduced to focus on the hard samples, which means the N_H^+ hardest positive samples with the lowest similarity and N_H^- hardest negative samples with the highest similarity in equation 7. Furthermore, the random sampling strategy is adopted to maintain global random contrast. There are N_R^- random negative samples selected to contrast with the input instance. In total, the sampling strategy adopted in our STD-CL takes contrast efficiency into account and contributes to the hard examples.

4 Experiment

4.1 Dataset Settings

NTU RGB+D. NTU RGB+D (NTU60) [Shahroudy *et al.*, 2016] is a large-scale dataset for skeleton-based action recog-

Table 2: Top-1 action acsification accuracy comparison (%) with the state-of-the-art methods on the NW-UCLA dataset. The numbers in gray indicate the results reported in their papers. Particularly, the 2S incidents the ensemble results of *joint* and *bone* streams. And the 4S incidents the ensemble results of *joint*, *bone*, *joint motion* and *bone motion* streams. * denotes the ensemble results of the streams reported in their papers.

Dataset Method/Streams	NW-UCLA			
	<i>J</i>	<i>B</i>	2S	4S
AGC-LSTM [Si <i>et al.</i> , 2019]	-	-	93.3*	-
DC-GCN+ADG [Cheng <i>et al.</i> , 2020a]	-	-	95.3	-
Shift-GCN [Cheng <i>et al.</i> , 2020b]	92.5	-	94.2	94.6
2S-AGCN [Shi <i>et al.</i> , 2019]	92.0	92.2	95.0	95.5
2S-AGCN w/STD-CL	93.8	93.1	95.9	97.0
CTR-GCN [Chen <i>et al.</i> , 2021a]	94.6	91.8	94.2	96.5
CTR-GCN w/STD-CL	94.8	94.6	95.7	97.2
InfoGCN [Chi <i>et al.</i> , 2022]	93.8	94.2	95.5	96.1
Info-GCN w/STD-CL	94.2	95.5	95.7	96.3
Hyperformer [Zhou <i>et al.</i> , 2022]	92.7	95.0	95.0	96.6
Hyperformer w/STD-CL	95.3	95.3	96.3	97.0

nition, which contains 56880 videos performed by 40 volunteers. The action sequences can be categorized into 60 classes. Following the authors of this dataset recommendation, we process this dataset into two benchmarks: cross-subject(X-sub) and cross-view(X-view). In the cross-subject setting, sequences of 20 subjects are for training, and the sequences of the rest 20 subjects are for validation. In the cross-view setting, skeleton sequences are split by camera views.

Samples from two camera views are used for training, and the rest are used for evaluation.

NTU RGB+D 120. NTU RGB+D 120 (NTU120) dataset [Liu *et al.*, 2019] adds 57367 new skeleton sequences and 60 new action classes to the original NTU RGB+D 60 dataset. There are 32 various video configurations in it, each of which depicts a different location and background. The authors offered the cross-subject(X-sub) and cross-setup(X-set) as two benchmark evaluations. In the cross-subject setting, sequences from 53 subjects are for training, and sequences from the other 53 subjects are for testing. In the cross-setup setting, skeleton sequences are split by setup ID. Samples from even set-up IDs are used for training, and the odd setup IDs are used for evaluation.

Northwestern-UCLA. Northwestern-UCLA (NW-UCLA) dataset [Wang *et al.*, 2014] contains 1494 video clips of 10 different actions captured from three Kinect cameras. We follow the same evaluation protocol in [Wang *et al.*, 2014]: the first two cameras for training and the other for testing.

Table 3: Top-1 accuracy comparison (%) with recent contrastive learning methods in supervised skeleton-based action recognition on the cross-subject benchmark of NTU120 dataset.

Method	Acc (%)
CTR-GCN [Chen <i>et al.</i> , 2021a]	84.9
GAP [Xiang <i>et al.</i> , 2023]	85.5
SkeletonGCL [Huang <i>et al.</i> , 2023]	85.6
FR Head [Zhou <i>et al.</i> , 2023]	85.5
STD-CL	85.5
STD-CL(Hyperformer [Zhou <i>et al.</i> , 2022])	86.8

4.2 Implementation Details

To fully validate the effectiveness and generalizability of STGCL, we take four different model-based approaches as baseline models. (1) CNN-based method. We select HCN [Li *et al.*, 2018] as the CNN-based method to validate STD-CL. We reproduce the experimental results using the released code and conduct our STD-CL on it. And we follow the training recipes as the paper describes. (2) GCN-based method. 2S-AGCN [Shi *et al.*, 2019] and CTR-GCN [Chen *et al.*, 2021a], the widely used GCN-based model for skeleton-based action recognition. For CTR-GCN, we follow their training strategies. Particularly, for 2S-AGCN, we update the training strategies from CTR-GCN, which can improve the performance significantly. (3) Transformer-based method. For transformer-based methods, we choose Hyperformer as the baseline.

For the details of contrastive learning, the size of the established memory banks is the length of the dataset. The dimensions of the decoupled features t and s is 256. For all datasets, the number of sampling instances N_H^+ , N_H^- and N_R^- are set as 128, 512, and 512, respectively. To select the model with the best performance, we experiment with temperatures τ of 0.5, 0.8, and 1.0. All experiments are conducted on four

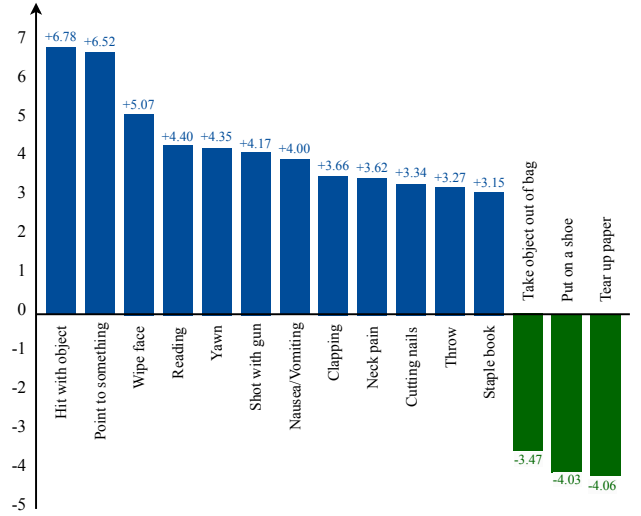


Figure 4: Action class with accuracy differences higher than 3% between CTR-GCN and our method in the cross-subject benchmark of NTU120 dataset.

GeForce GTX NVIDIA 3090 GPUs. **More implementation details are presented in the supplementary material.**

4.3 Comparison With The State-of-The-Art

We compare our method with previous SOTA methods in Tables 1 and 2. To fully validate the effectiveness of the proposed STD-CL, we compare the experimental results in a single modality and the ensemble results of multi-modality. J means the *joint* stream, B denotes the *bone* stream, $2S$ denotes the ensemble results of the above two streams in default, and $4S$ incidents the ensemble results of additional *joint motion* and *bone motion* streams. Particularly, due to the design of their model architecture, the experimental results of VALSTM [Zhang *et al.*, 2017], ACG-LSTM [Si *et al.*, 2019] and HCN [Li *et al.*, 2018] are the ensemble results of two streams. Therefore, we classify the results into $2S$.

As shown in Table 1, on NTU60 and NTU120, combined with STD-CL, all four various baselines achieve solid gains on these four benchmarks of the two datasets over different settings. Moreover, the improvement in a single stream can be generalized to the results of the multi-stream ensemble. Take CTR-AGCN as an example, it improves by 0.6% (89.8% to 90.4%) in the joint stream, 0.6% (90.2% to 90.8%) in the bone stream, and 0.2% (92.0% to 92.2%) in their fusion result.

As shown in Table 2, on NW-UCLA, STD-CL outperforms 2S-AGCN by 1.5%. It also outperforms CTR-CCN by 0.7%. And it outperforms the recent work InfoGCN and Hyperformer by 0.2% and 0.4%, respectively. Considering that the performance on this dataset is already very high, such improvement brought by STD-CL is significant.

4.4 Comparison With Other Contrastive Learning Method

We compare our method with the recent contrastive learning methods in supervised skeleton-based action recogni-

(a) Impact of the channel reduction rate in STFD.

Method	r	Acc(%)
CTR-GCN	-	84.9
	4	-
	8	85.5
	16	-

(b) Impact of the dimension of the decoupled features.

Method	D	Acc(%)
CTR-GCN	-	84.9
	128	-
	256	85.5
	512	-

(c) Contrastive strategies

Method	Acc(%)
Baseline (w/o contrast)	84.9
w/SD-CL	-
w/TD-CL	-
w/G-CL	-
w/STD-CL w/ G-CL	-
STD-CL	85.5

(d) Accuracy on different level actions.

Setting	Acc(%)		
Method/Level	Hard	Medium	Easy
2S-AGCN	65.0	86.2	95.1
2S-AGCN w/o ours	65.9 ^{↑0.9}	86.6 ^{↑0.4}	95.2 ^{↑0.1}
CTR-AGCN	65.9	85.8	95.4
CTR-AGCN w/o ours	66.1 ^{↑0.2}	87.0 ^{↑1.2}	95.9 ^{↑0.5}
Hyperformer	68.3	85.9	95.2
Hyperformer w/o ours	69.6 ^{↑1.3}	87.0 ^{↑1.1}	95.4 ^{↑0.2}

(e) The comparison of training consumption.

Method	Memory-Usage (G)	Time (min/epoch)
HCN	-	-
HCN w/o ours	-	-
2S-AGCN	-	-
2S-AGCN w/o ours	-	-
CTR-AGCN	-	-
CTR-AGCN w/o ours	-	-
Hyperformer	-	-
Hyperformer w/o ours	-	-

Table 4: Ablation study with different experimental settings of STD-CL on NTU120. The Acc incidents the accuracy of the action recognition. SD-CL means applying spatial decoupled features to contrastive learning, and TD-CL means applying temporal decoupled features to contrastive learning. G-CL means applying the global features, which is the output of the global mean pooling layer, to contrastive learning.

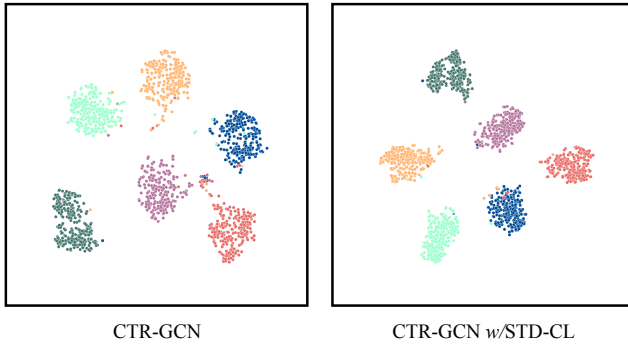


Figure 5: Visualization of feature representation by t-SNE from the sequences from sequences in the test set of the cross-subject benchmark of NTU120 dataset. Different colors denote different classes. The left one is from the CTR-GCN, while the right one is from our method.

tion. The comparison is conducted on the cross-subject of the NTU120 dataset. As shown in Table 3, our STD-CL achieves competitive improvements. Furthermore, most previous methods are only compatible with GCN-based methods. To take advantage of our method, we combine the STD-CL with Hyperformer, which is a transformer-based method. Our method outperforms previous contrastive learning methods by 1.2%, which is a promising result. **For more comparisons, please refer to the supplementary materials.**

4.5 Ablation Study

In this section, we conduct experiments to evaluate the different experimental settings on the cross-subject benchmark of the NTU120 dataset to verify the design of the proposed STD-CL. The experimental results of ablation studies are shown in

Table 4.

Hyperparameter in STFD module. Table 4 (a) studies the impact of the channel reduction rate r , we try .

Contrastive strategies.

Performance on different level actions. To evaluate the effectiveness of the proposed STD-CL, we conduct recognition accuracy for different action categories with different levels of difficulty. Specifically, we gather actions whose accuracy is over 90% as Easy Level, between 80% to 90% as Medium Level, and lower than 80% as Hard Level for their respective classification results. The experimental results are displayed in Table 4 (d). From the results, we can observe that the proposed STD-CL achieves relatively significant improvements in the hard and medium-level actions, which include more fine-grained action categories. Moreover, the proposed STD-CL has made some gains in the easy-level actions, thanks to the explicit modeling for the latent data distributions of contrastive learning.

Furthermore, we compare our results with a SOTA model CTR-GCN [Chen *et al.*, 2021a], and the results of class with accuracy differences higher than 3% between CTR-GCN and our method are displayed in Figure 4. We can observe that actions such as "hit with object", "point to something", "wipe face", "reading" and "yawn" benefit from the proposed STD-CL due to the great capacity to obtain discriminative and semantically distinct features. Besides, the reason for the poor performance of actions "take object out of bag", "put on a shoe", and "tear up paper" is that such actions are strongly object-related, making it challenging to recognize and contrast.

Training consumption.

4.6 Qualitative Analysis

In this section, we validate our STD-CL through t-SNE distribution visualization of feature representations in the test set of the cross-subject benchmark of the NTU120 dataset. As shown in Figure 5, our STD-CL can exploit the data distributions explicitly with more compact intra-class distances and clear classification boundaries. Thus, the features extracted from the proposed STD-CL are more discriminative, which shows that the decoupled feature contrast improves the feature extraction capacity of the skeleton encoders.

5 Conclusion

In this paper, we propose a novel spatial-temporal decoupling contrastive learning (STD-CL) framework for skeleton-based action recognition, which can be combined with most of the previous skeleton encoders. We employ contrastive learning for the spatial and temporal decoupled features to encourage the skeleton encoders to extract more discriminative and semantically distinct features, which are proven to be effective for recognizing fine-grained action classes and ambiguous samples. The extensive experimental results with four various skeleton encoders on three datasets demonstrate the effectiveness of the proposed framework.

References

- [Cao *et al.*, 2017] Zhe Cao, Tomas Simon, Shih-En Wei, and Yaser Sheikh. Realtime multi-person 2d pose estimation using part affinity fields. In *Proceedings of the IEEE Conference on Computer Vision and Pattern Recognition*, pages 7291–7299, 2017.
- [Chen *et al.*, 2020] Ting Chen, Simon Kornblith, Mohammad Norouzi, and Geoffrey Hinton. A simple framework for contrastive learning of visual representations. In *Proceedings of the International Conference on Machine Learning*, pages 1597–1607. PMLR, 2020.
- [Chen *et al.*, 2021a] Yuxin Chen, Ziqi Zhang, Chunfeng Yuan, Bing Li, Ying Deng, and Weiming Hu. Channel-wise topology refinement graph convolution for skeleton-based action recognition. In *Proceedings of the IEEE International Conference on Computer Vision*, pages 13359–13368, 2021.
- [Chen *et al.*, 2021b] Zhan Chen, Sicheng Li, Bing Yang, Qinghan Li, and Hong Liu. Multi-scale spatial temporal graph convolutional network for skeleton-based action recognition. In *Proceedings of the AAAI Conference on Artificial Intelligence*, volume 35, pages 1113–1122, 2021.
- [Cheng *et al.*, 2020a] Ke Cheng, Yifan Zhang, Congqi Cao, Lei Shi, Jian Cheng, and Hanqing Lu. Decoupling gcw with dropgraph module for skeleton-based action recognition. In *Proceedings of the European Conference on Computer Vision*, pages 536–553. Springer, 2020.
- [Cheng *et al.*, 2020b] Ke Cheng, Yifan Zhang, Xiangyu He, Weihang Chen, Jian Cheng, and Hanqing Lu. Skeleton-based action recognition with shift graph convolutional network. In *Proceedings of the IEEE Conference on Computer Vision and Pattern Recognition*, pages 183–192, 2020.
- [Chi *et al.*, 2022] Hyung-gun Chi, Myoung Hoon Ha, Seunggeun Chi, Sang Wan Lee, Qixing Huang, and Karthik Ramani. Infocn: Representation learning for human skeleton-based action recognition. In *Proceedings of the IEEE Conference on Computer Vision and Pattern Recognition*, pages 20186–20196, 2022.
- [Dang *et al.*, 2019] Qi Dang, Jianqin Yin, Bin Wang, and Wenqing Zheng. Deep learning based 2d human pose estimation: A survey. *Tsinghua Science and Technology*, 24(6):663–676, 2019.
- [Du *et al.*, 2015] Yong Du, Wei Wang, and Liang Wang. Hierarchical recurrent neural network for skeleton based action recognition. In *Proceedings of the IEEE Conference on Computer Vision and Pattern Recognition*, pages 1110–1118, 2015.
- [He *et al.*, 2020] Kaiming He, Haoqi Fan, Yuxin Wu, Saining Xie, and Ross Girshick. Momentum contrast for unsupervised visual representation learning. In *Proceedings of the IEEE Conference on Computer Vision and Pattern Recognition*, pages 9729–9738, 2020.
- [Huang *et al.*, 2023] Xiaohu Huang, Hao Zhou, Bin Feng, Xinggang Wang, Wenyu Liu, Jian Wang, Haocheng Feng, Junyu Han, Errui Ding, and Jingdong Wang. Graph contrastive learning for skeleton-based action recognition. 2023.
- [Li *et al.*, 2018] Chao Li, Qiaoyong Zhong, Di Xie, and Shiliang Pu. Co-occurrence feature learning from skeleton data for action recognition and detection with hierarchical aggregation. *Proceedings of the International Joint Conference on Artificial Intelligence*, 2018.
- [Liu *et al.*, 2019] Jun Liu, Amir Shahroudy, Mauricio Perez, Gang Wang, Ling-Yu Duan, and Alex C Kot. Ntu rgb+ d 120: A large-scale benchmark for 3d human activity understanding. *IEEE Transactions on Pattern Analysis and Machine Intelligence*, 42(10):2684–2701, 2019.
- [Liu *et al.*, 2020] Ziyu Liu, Hongwen Zhang, Zhenghao Chen, Zhiyong Wang, and Wanli Ouyang. Disentangling and unifying graph convolutions for skeleton-based action recognition. In *Proceedings of the IEEE Conference on Computer Vision and Pattern Recognition*, pages 143–152, 2020.
- [Plizzari *et al.*, 2021] Chiara Plizzari, Marco Cannici, and Matteo Matteucci. Spatial temporal transformer network for skeleton-based action recognition. In *Pattern Recognition. ICPR International Workshops and Challenges: Virtual Event, January 10–15, 2021*, pages 694–701. Springer, 2021.
- [Ren *et al.*, 2020] Bin Ren, Mengyuan Liu, Runwei Ding, and Hong Liu. A survey on 3d skeleton-based action recognition using learning method. *arXiv preprint arXiv:2002.05907*, 2020.
- [Shahroudy *et al.*, 2016] Amir Shahroudy, Jun Liu, Tian-Tsong Ng, and Gang Wang. Ntu rgb+ d: A large scale

- dataset for 3d human activity analysis. In *Proceedings of the IEEE Conference on Computer Vision and Pattern Recognition*, pages 1010–1019, 2016.
- [Shi *et al.*, 2019] Lei Shi, Yifan Zhang, Jian Cheng, and Hanqing Lu. Two-stream adaptive graph convolutional networks for skeleton-based action recognition. In *Proceedings of the IEEE Conference on Computer Vision and Pattern Recognition*, pages 12026–12035, 2019.
- [Shi *et al.*, 2020] Lei Shi, Yifan Zhang, Jian Cheng, and Hanqing Lu. Decoupled spatial-temporal attention network for skeleton-based action-gesture recognition. In *Proceedings of the Asian Conference on Computer Vision*, 2020.
- [Si *et al.*, 2019] Chenyang Si, Wentao Chen, Wei Wang, Liang Wang, and Tieniu Tan. An attention enhanced graph convolutional lstm network for skeleton-based action recognition. In *Proceedings of the IEEE Conference on Computer Vision and Pattern Recognition*, pages 1227–1236, 2019.
- [Song *et al.*, 2017] Sijie Song, Cuiling Lan, Junliang Xing, Wenjun Zeng, and Jiaying Liu. An end-to-end spatio-temporal attention model for human action recognition from skeleton data. In *Proceedings of the AAAI Conference on Artificial Intelligence*, volume 31, 2017.
- [Song *et al.*, 2022] Yi-Fan Song, Zhang Zhang, Caifeng Shan, and Liang Wang. Constructing stronger and faster baselines for skeleton-based action recognition. *IEEE Transactions on Pattern Analysis and Machine Intelligence*, 45(2):1474–1488, 2022.
- [Wang *et al.*, 2014] Jiang Wang, Xiaohan Nie, Yin Xia, Ying Wu, and Song-Chun Zhu. Cross-view action modeling, learning and recognition. In *Proceedings of the IEEE Conference on Computer Vision and Pattern Recognition*, pages 2649–2656, 2014.
- [Wu *et al.*, 2018] Zhirong Wu, Yuanjun Xiong, Stella X Yu, and Dahua Lin. Unsupervised feature learning via non-parametric instance discrimination. In *Proceedings of the IEEE Conference on Computer Vision and Pattern Recognition*, pages 3733–3742, 2018.
- [Xiang *et al.*, 2023] Wangmeng Xiang, Chao Li, Yuxuan Zhou, Biao Wang, and Lei Zhang. Generative action description prompts for skeleton-based action recognition. In *Proceedings of the IEEE International Conference on Computer Vision*, pages 10276–10285, 2023.
- [Xu *et al.*, 2022] Kailin Xu, Fanfan Ye, Qiaoyong Zhong, and Di Xie. Topology-aware convolutional neural network for efficient skeleton-based action recognition. In *Proceedings of the AAAI Conference on Artificial Intelligence*, volume 36, pages 2866–2874, 2022.
- [Xu *et al.*, 2023] Binqian Xu, Xiangbo Shu, Jiachao Zhang, Guangzhao Dai, and Yan Song. Spatiotemporal decouple-and-squeeze contrastive learning for semisupervised skeleton-based action recognition. *IEEE Transactions on Neural Networks and Learning Systems*, 2023.
- [Yan *et al.*, 2018] Sijie Yan, Yuanjun Xiong, and Dahua Lin. Spatial temporal graph convolutional networks for skeleton-based action recognition. In *Proceedings of the AAAI Conference on Artificial Intelligence*, volume 32, 2018.
- [Ye *et al.*, 2020] Fanfan Ye, Shiliang Pu, Qiaoyong Zhong, Chao Li, Di Xie, and Huiming Tang. Dynamic gcn: Context-enriched topology learning for skeleton-based action recognition. In *Proceedings of the ACM International Conference on Multimedia*, pages 55–63, 2020.
- [Zhang *et al.*, 2017] Pengfei Zhang, Cuiling Lan, Junliang Xing, Wenjun Zeng, Jianru Xue, and Nanning Zheng. View adaptive recurrent neural networks for high performance human action recognition from skeleton data. In *Proceedings of the IEEE International Conference on Computer Vision*, pages 2117–2126, 2017.
- [Zhang *et al.*, 2019] Hong-Bo Zhang, Yi-Xiang Zhang, Bineng Zhong, Qing Lei, Lijie Yang, Ji-Xiang Du, and Duan-Sheng Chen. A comprehensive survey of vision-based human action recognition methods. *Sensors*, 19(5):1005, 2019.
- [Zhang *et al.*, 2020] Pengfei Zhang, Cuiling Lan, Wenjun Zeng, Junliang Xing, Jianru Xue, and Nanning Zheng. Semantics-guided neural networks for efficient skeleton-based human action recognition. In *proceedings of the IEEE Conference on Computer Vision and Pattern Recognition*, pages 1112–1121, 2020.
- [Zhou *et al.*, 2022] Yuxuan Zhou, Zhi-Qi Cheng, Chao Li, Yanwen Fang, Yifeng Geng, Xuansong Xie, and Margret Keuper. Hypergraph transformer for skeleton-based action recognition. *arXiv preprint arXiv:2211.09590*, 2022.
- [Zhou *et al.*, 2023] Huanyu Zhou, Qingjie Liu, and Yunhong Wang. Learning discriminative representations for skeleton-based action recognition. In *Proceedings of the IEEE Conference on Computer Vision and Pattern Recognition*, pages 10608–10617, 2023.